CHAPTER 4

THE NOTCH-TOUGHNESS OF WELDED 3CR12 AND 3CR12Ni

SYNOPSIS

The newly developed bead-on-plate bend test was used to determine the influence of the narrow, coarse grained, high temperature weld heat affected zone (HT HAZ) on the fusion line fracture behaviour of bead-on-plate welds on 6.2 mm 3CR12 and 3CRNi plate. The weld fusion line fracture toughness is characterized in terms of a fracture appearance transition temperature (FATT). The influence of factors like the phase composition of the HT HAZ, base and weld metal strength, punch speed during bend testing and the weld fusion line orientation of the bead-on-plate bend specimens, on the fusion line fracture behaviour, was determined.

The actural FATT of the HT HAZ of bead-on-plate welds on 6.2 mm plate are higher than the maximum values of 106°C and 120°C which were obtained in this study for 3CR12 and 3CRNi, respectively. This is due to a fracture mode transition at the FATT from cleavage fracture in the HT HAZ to ductile tearing in the fine grained and low temperature HAZ. This transition is explained in terms of the Davidenkov-Ludwik fracture theory.

The HT HAZ fracture toughness of welds on 3CR12 and 3CR12Ni is lower than both the values reported in the literature for respectively the weld HAZ of 3CR12 and AISI 409. It was not improved significantly by a marked decrease in the grain size of this zone from ASTM No. 1-2 to a fine, low carbon, martensitic structure associated with an increase in the martensite content from 15 percent to 98 percent. The fracture toughness of the HT HAZ is therefore probably determined by other phenomena which has not yet been identified.

The effect of the weld heat input of bead-on-plate MMA welds on 11 mm thick 3CR12 plate, within the range of 0.64 - 1.81 kJ/mm, was to increase the width of the HT HAZ from 0.41 mm to 1.1 mm; the phase composition and grain size were unchanged. The phase composition of the HT HAZ is not only dependent on the ferrite factor but is also dependent on the Ti/(C+N) ratio and the thermomechanical history of the steel.

The influence of the base and weld metal strength on the fusion line fracture behaviour of bead-on-plate welds on 6.2 mm thick 3CR12 plate cannot be determined using the newly developed bead-on-plate bend test. This is attributed to the high constraint offered alone by the large welding bead.

THE NOTCH-TOUGHNESS OF WELDED 3CR12 AND 3CR12Ni

1. INTRODUCTION

The probability of the HT HAZ fracture toughness of 3CR12 being much lower than generally reported in the literature, has already been pointed out in the chapter one. The very low HT HAZ fracture toughness values which were obtained for the 14 percent chromium steels as well as the fact that these values were not significantly influenced by large fractions low carbon martensite and the fact that 3CR12 has a much lower nickel content (0.6%), strongly suggest that the HT HAZ fracture toughness of 3CR12 is not significantly higher than that of AISI 409.

The very low HT HAZ fracture toughness values which were obtained in the previous chapter can be attributed to the fact that the bead-on-plate bend test is a very severe test. The weld HAZ was subjected to very high levels of constraint during bend testing due to inter alia the high strength of the hot rolled base plate. It has also been shown that the weld fusion line fracture behaviour of the 14% chromium steels are strongly dependent on the weld metal mechanical properties. Recently, a new filler metal, designated E3CR12, became available on the market exclusively for welding of 3CR12.

With reference to the abovementioned aspects, it was decided to study the effects of the following factors on the fusion line fracture behaviour of welds on 3CR12 and 3CR12Ni. For this purpose the newly developed bead-on-plate bend test was used.

a. Phase composition of the HT HAZ
b. Base metal strength
c. Weld metal strength (AISI 316L weld metal vs E3CR12)
d. Loading rate or punch speed during bend testing
e. Orientation of the fusion line of bead-on-plate welds relative to the plate surface

2. EXPERIMENTAL PROCEDURE

2.1 Chemical compositions

In order to determine the effect of the phase composition on the fusion line fracture behaviour of welds on 3CR12, two experimental steels (Table 4.1) with respectively 45 (3CR12) and 100 percent martensite (3CR12Ni) in the HT HAZ were designed using Kaltenhauser's ferrite factor and the design curve in figure 4.1 which was determined in a previous study(1,23). Superimposed on this curve are also the curves which were obtained by Middelburg Steel and Alloys (Pty), Ltd. and Eckenrod and Kovach(24) for respectively 3CR12 and a 11.5 percent chromium, 0.85 nickel steel (Crucible E-4).

The experimental steels were supplied by Middelburg Steel and Alloys (Pty), Ltd. in two conditions, i.e. 6.2 mm hot rolled 3CR12 and 3CR12Ni plate and 6.2 mm tempered 3CR12 and 3CR12Ni plate. Final hot rolling was executed at 820-850°C followed by air cooling. Tempering was done at 780°C for 20 minutes.

Table 4.1: Chemical compositions (wt-%) of experimental 3CR12 and 3CR12Ni steels.

Steel	C	S	P	Mn	Si	Ti	Cr	Ni	N	F.F*
3CR12	0.027	0.008	0.020	1.32	0.44	0.32	11.34	0.60	0.022	9.54
3CR12Ni	0.025	0.011	0.027	0.94	0.49	0.22	11.53	1.19	0.018	7.87

*F.F.: Ferrite factor

2.2 Specimen preparation

The design of the bead-on-plate bend test specimen for evaluating the fusion line notch fracture toughness of welds on 3CR12 and 3CR14, has already been discussed in detail in chapter 3.

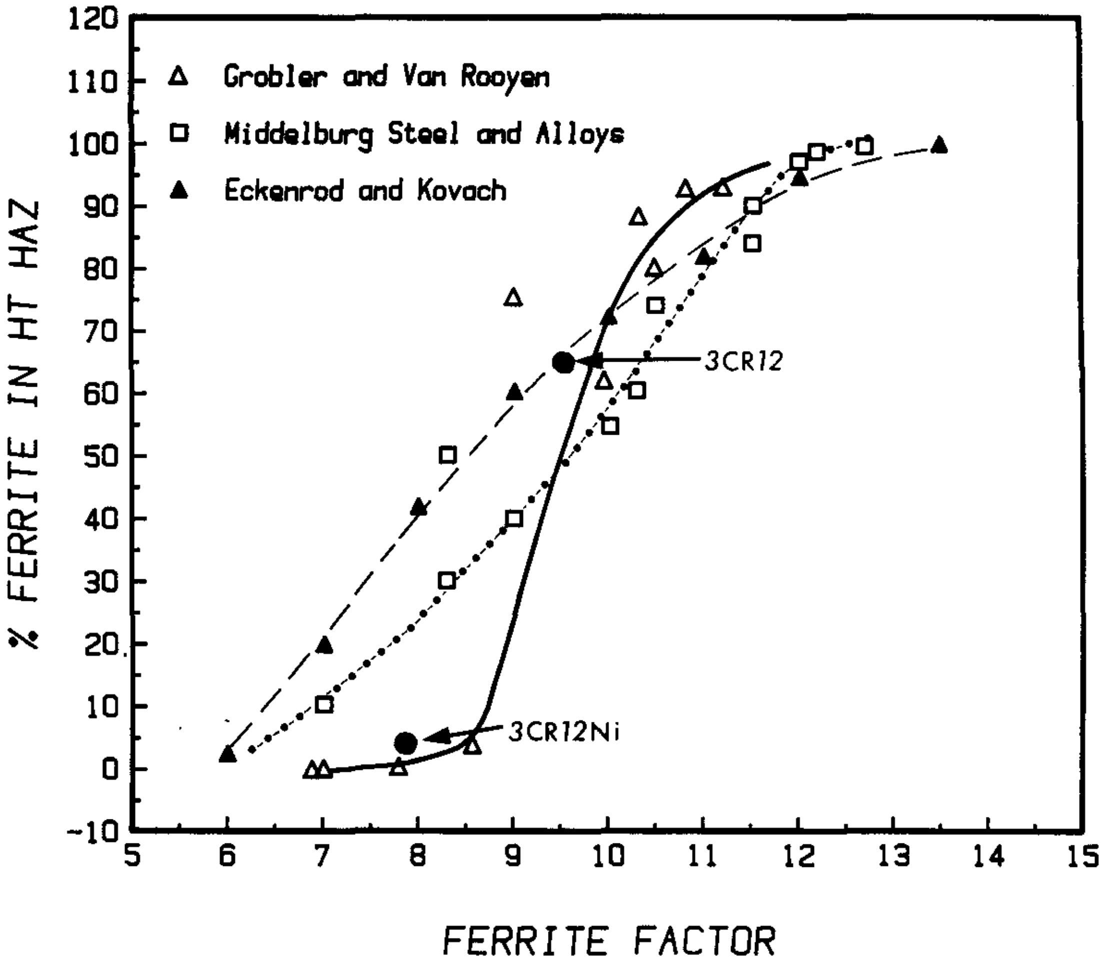

Figure 4.1: Percentage ferrite in the HT HAZ of 3CR12 and 3CR12Ni versus the ferrite factor. The HT HAZ phase composition of the experimental 3CR12Ni and 3CR12 steels are indicated.

Bead-on-plate bend specimens (fig. 3.2) were prepared from respectively 6.2 mm hot rolled and tempered plate, using two different filler metals, viz AISI 316L and E3CR12. The bead-on-plate welds were welded according to the following welding parameters:

Welding process	:	MIG
Welding position	:	Flat
Welding wire	:	1.6 mm dia. AISI 316L
	:	1.6 mm dia. flux cored E3CR12
Current (ampere)	:	370-380
Volts	:	20-21
Welding speed (cm/min.)	:	95 (316L)
	:	90 (E3CR12)
Welding gas	:	84% Ar, 13% CO_2 and 3% O_2.

In order to obtain the excessively large welding bead together with the deep penetration (fig. 3.3) a special shielding gas (84%Ar, 13%CO_2 and 3%O_2) was used. The weld metal carbon content increased slightly due to carbon pick-up from the CO_2 in the shielding gas. Table 4.2 show the weld metal chemical analysis of MIG welds which were welded with respectively the abovementioned shielding gas and a gas which contained only 98%Ar and 2%O_2. The increase in weld metal carbon content from 0.014% to 0.044% will result in an increase in the weld metal yield strength. The HT HAZ may therefore, as a result of this higher weld metal yield strength, be subjected to slightly higher constraints during bend testing.

Table 4.2: Weld metal (316L) chemical analysis of MIG welds (multi-layer cladded specimen), welded respectively with shielding gasses which contained (84%Ar, 13%CO_2, 3%O_2) and (98%Ar, 2%O_2).

Shielding gas	C	P	Mn	Ni	Cr	Mo	Si
84%Ar, 13%CO_2,3%O_2	0.044	0.02	1.17	11.8	18.2	2.4	0.25
98%Ar, 2%O_2	0.014	0.02	1.35	11.9	18.6	2.5	0.28

3. EXPERIMENTAL RESULTS

3.1 Microstructures

Figure 4.2 shows the coarse grained, duplex ferrite-martensite microstructure of the HT HAZ of bead-on-plate welds on respectively hot rolled and tempered 6.2 mm 3CR12 plate. The HT HAZ of the tempered specimen exhibits a much higher martensite content compared to the hot rolled specimen. No significant differences were observed in the HT HAZ microstructures of the hot rolled and tempered 3CR12Ni specimens (fig. 4.3). The phase compositions of the HT HAZ's of the bead-on-plate bend test specimens, are summarized in table 4.3. It was determined by an area analysis from photographs which were prepared using both high contrast film and printing paper. The width of the HT HAZ ranged from 0.25 mm to 0.35 mm.

Table 4.3: Phase composition of the HT HAZ of bead-on-plate welds on 6.2 mm 3CR12 and 3CR12Ni plate.

Steel	Condition	% Martensite in HT HAZ
3CR12	Hot rolled	15
3CR12	Hot rolled and tempered	35
3CR12Ni	Hot rolled	97
3CR12Ni	Hot rolled and tempered	96

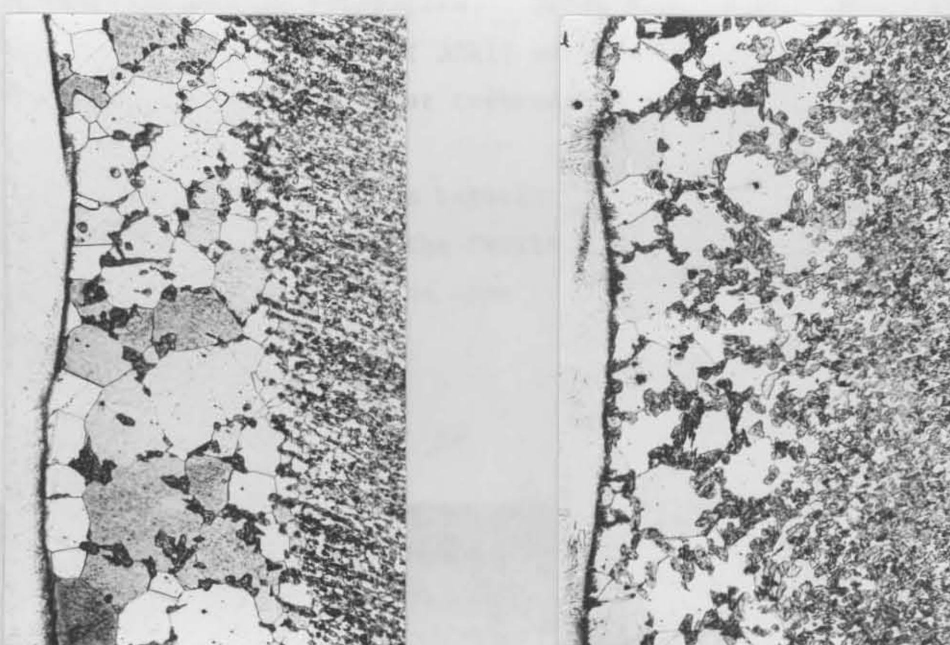

a. b.

Figure 4.2: Coarse grained, ferrite-martensite microstructure of the HT HAZ of bead-on-plate welds on 6.2 mm 3CR12 plate (160X).

a. Hot rolled plate

b. Hot rolled and tempered plate

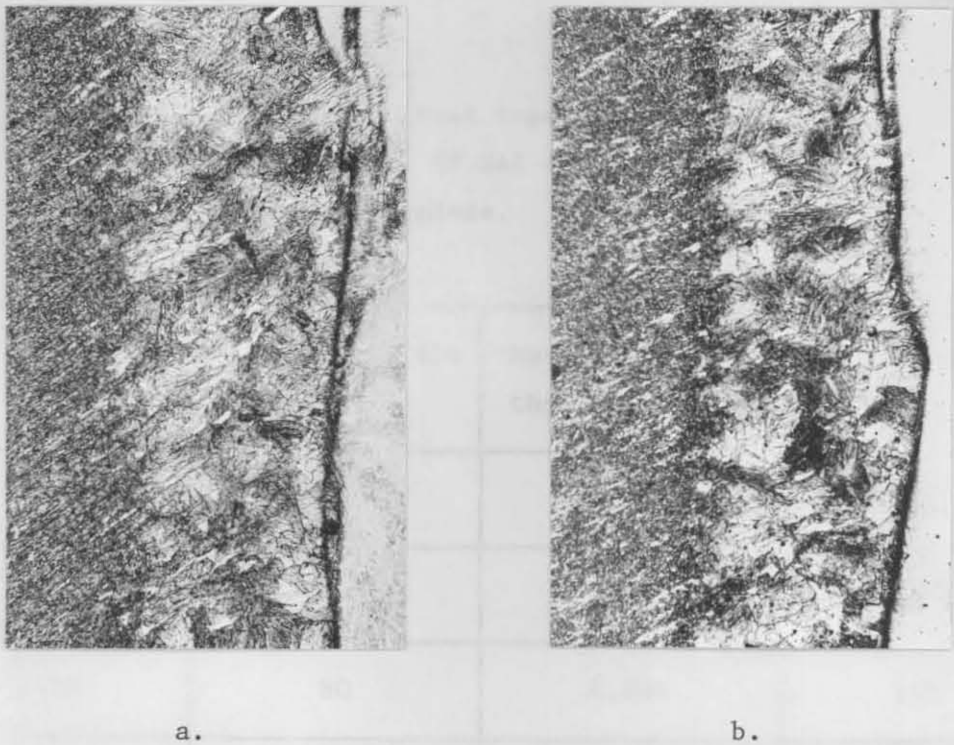

Figure 4.3: Duplex ferrite-martensite microstructure of the HT HAZ of bead-on-plate welds on 6.2 mm 3CR12Ni plate (160X).
a. Hot rolled plate
b. Hot rolled and tempered plate

The phase compositions of the HT HAZ of the tempered 3CR12 and 3CRNi specimens are superimposed on figure 4.1. Figure 4.1 shows that the phase composition of the HT HAZ of MIG welds on 3CR12 may be accurately predicted using Grobler and Van Rooyen's design curve which was constructed using the MIG welding process. The other curves were constructed using both the MMA and MIG welding processes. The differences between the curves, especially at ferrite factors below 9.5 may be attributed partly to the fact that the steels which were used to determine these curves were not subjected to the same prior thermomechanical treatments. Table 4.3, e.g., shows that the martensite content of the HT HAZ of 3CR12 was increased from 15 percent to 35 percent by a prior tempering heat treatment subsequent to hot rolling.

Another reason for the differences between the curves in figure 4.1 may be the fact that the formula for the ferrite factor includes the total titanium, carbon and nitrogen in the steel, while the percentage ferrite in the HT HAZ is determined by the dissolved titanium, carbon and nitrogen rather than by the total percentages. The dissolved titanium, carbon and nitrogen in the HT HAZ is determined by the Ti/(C+N) ratio which was not the same for the experimental steels which were used to construct the different curves in figure 4.1.

Since the microstructure of the HT HAZ originates during non-equilibrium heating and cooling cycles, the fraction δ-ferrite which will transform into austenite during the weld cooling cycle is determined, inter alia by the cooling rate. The cooling rate is determined by the welding process, the section thickness, joint design and the heat input during welding. The effect of heat input on the phase composition, width, and grain size, of the HT HAZ was determined in this study by preparing bead-on-plate MMA welded specimens from 10 mm commercial 3CR12 plate. The specimens were welded with a 3.25 mm diameter AISI 309L electrode at heat inputs ranging from 0.64 kJ/mm to 1.81 kJ/mm. The results are summarized in table 4.4 and figure 4.4.

Table 4.4: The effect of the weld heat input on the ferrite content, width and grain size of the HT HAZ of bead-on-plate welds on 10 mm thick commercial 3CR12 plate.

Weld heat input (kJ/mm)	% Ferrite in the HT HAZ	Max. width of the HT HAZ (mm)	ASTM grain size No.
0.64	81	0.406	2-3
0.97	82	0.742	1-2
1.25	80	0.802	1-2
1.36	77	0.902	1-2
1.51	78	1.043	1-2
1.81	79	1.063	1-2

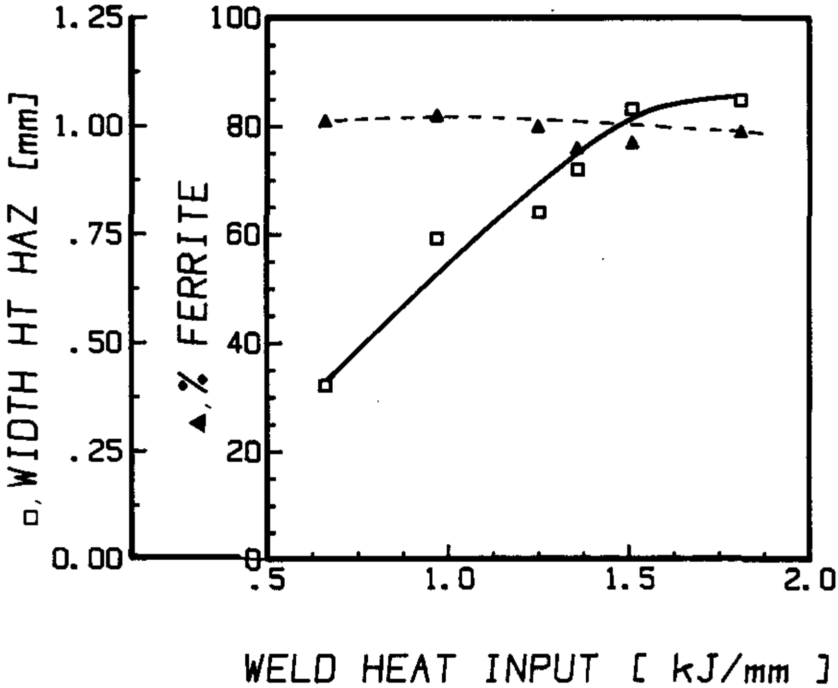

Figure 4.4: Phase composition and width of the HT HAZ of 3CR12 versus heat input for MMA welding.

Figure 4.4 shows that variation of the heat input only increases the size of the HT HAZ while the phase composition and grain size are unchanged. This may be explained as follows: Partial transformation of δ-ferrite to austenite occurs, during cooling from the solidus temperature, within the temperature range of about 1300°C to 1000°C (fig. 1.2). The resultant variations in thermal cycle which were obtained in this temperature range by welding within the heat input range of 0.64 to 1.81 kJ/mm had very little influence on the fraction δ-ferrite which transformed to austenite during cooling.

It may therefore be concluded that the phase composition of the HT HAZ of welds on 3CR12, over the range of heat inputs appropriate to manual welding (i.e. 0.6 to 1.6 kJ/mm), is determined mainly by the thermomechanical history, chemical composition and Ti/(C+N) ratio of the steel.

3.2 The influence of the phase composition of the HT HAZ, loading rate, the weld metal and base metal strength on the fusion line notch fracture toughness of 3CR12 and 3CR12Ni

The effect of the phase composition of the HT HAZ on the fusion line fracture behaviour was determined by comparing the bead-on-plate bend test results of specimens prepared from respectively 3CR12 and 3CR12Ni plate. The effect of weld metal strength was determined by comparing the test results of specimens welded respectively with a low strength AISI 316L filler metal and a high strength E3CR12 filler metal, while the effect of the base metal strength was determined by comparing test results of specimens prepared respectively from hot rolled and hot rolled-and-tempered plate.

The influences of the abovementioned variables on the fracture behaviour of welds were determined at a punch speed of 133 mm/min. during three point

Table 4.5: Bead-on-plate bend test results for 3CR12 and 3CR12Ni.

Steel	Condition A: Hot rolled B: & tempered	Filler metal	% martensite in HT HAZ	Bend testing (133mm/min)		Charpy impact loading		Vickers hardness	
				FATT (°C)	Frac. Mode*	FATT (°C)	Frac. Mode*	Weld metal	Base metal
3CR12Ni	A	316L	97	77	1	98	4	220	322
3CR12Ni	A	E3CR12	97	70	2	106	2	283	322
3CR12Ni	B	316L	96	69	2	36	2	282	196
3CR12	A	316L	15	92	3	104	2	277	246
3CR12	A	E3CR12	15	106	3	120	2	374	246
3CR12	B	316L	35	105	2	106	3	311	165

* Fracture mode transition at FATT:

1. Ductile - cleavage fracture in HT weld HAZ.
2. Cleavage fracture in HT weld HAZ at T < FATT.
   Ductile tearing in fine grained and low temperature HAZ at T > FATT.
3. Cleavage fracture in HT weld HAZ at T < FATT.
   90° bend without fracture at T > FATT.
4. Cleavage fracture in HT weld HAZ at T < FATT.
   Ductile fracture in HT weld HAZ and weld metal at T > FATT.

face bend testing. The effect of loading rate or punch speed was determined at punch speeds ranging from 2 mm/min. to 430 mm/min. Some specimens were also tested by impact loading in a Charpy impact machine. The results of this study is summarized in table 4.5.

3.2.1 3CR12Ni steel weld fracture behaviour

The hot rolled 3CR12Ni bend specimens welded with an AISI 316L filler metal, and which contained 97 percent martensite in the HT HAZ, fractured exclusively in the HT HAZ adjacent to the fusion line. Figure 4.5 shows a brittle cleavage fracture in this zone of a specimen tested at 50°C while figure 4.6 shows a ductile fracture in this zone of a specimen tested at 95°C.

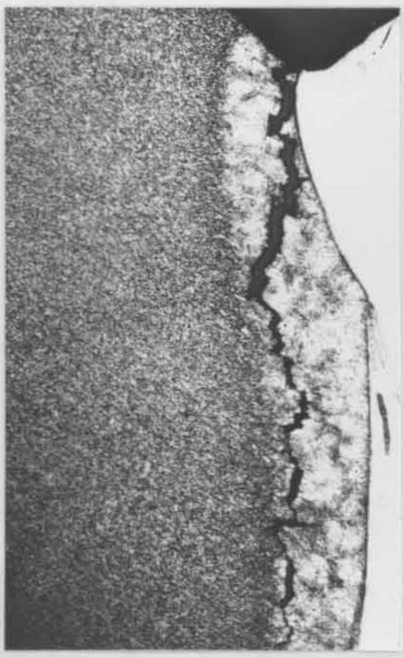

Figure 4.5: Brittle cleavage fracture in the HT HAZ of a bead-on-plate bent specimen, prepared from hot rolled 3CR12Ni plate and tested at 50°C (35X).

Figure 4.6: Ductile fracture in the HT HAZ of a bead-on-plate bent specimen, prepared from hot rolled 3CR12Ni plate and tested at 95°C (35X).

The FATT was determined by a fracture surface analysis of only that part of the fracture surface where the crack path was limited to the HT HAZ. The fracture surfaces of the bent specimens together with the FATT curve is shown in figure 4.7. A FATT of 77°C (at 50 percent ductile fracture surface) was obtained for the HT HAZ of hot rolled 3CR12Ni specimens welded with a AISI 316L filler metal.

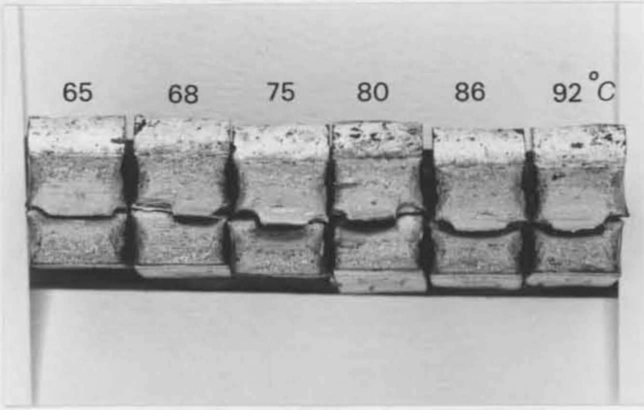

a.

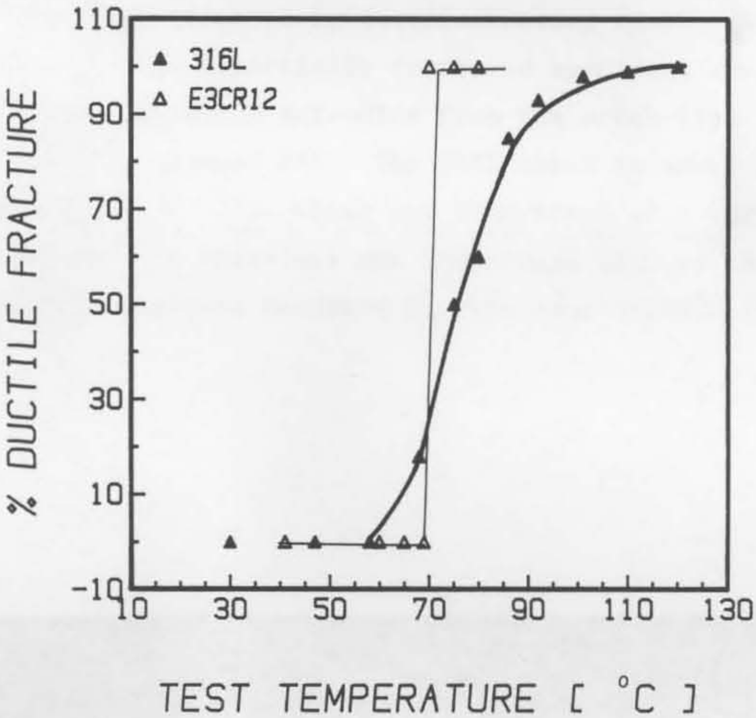

b.

Figure 4.7: a. Fracture surfaces of hot rolled 3CR12Ni bead-on-plate bent specimens welded with an AISI 316L filler metal. Test temperatures (°C) are indicated.

b. FATT curves for hot rolled 3CR12Ni specimens welded respectively with AISI 316L and E3CR12 filler metals.

In some of the bead-on-plate bend specimens the notch tip was not positioned exactly on the fusion line, but displaced slightly towards the weld metal (fig. 4.8). Even with the notch in this position, both brittle and ductile fractures were limited to the HT HAZ. Figure 4.8 shows a partially fractured specimen with a short ductile crack which propagated for a distance of only 0.15 mm in the weld metal. The possibility that this crack initiated in the HT HAZ rather than in the weld metal has already been discussed in the previous chapter.

Figure 4.8: Partially fractured bead-on-plate 3CR12Ni bent specimen with the notch tip located in the weld metal. Note the short ductile crack (specimen tested at 90°C) extending from the notch tip through the weld metal into the HT HAZ (75X).

The hot rolled 3CR12Ni specimens welded with the high strength E3CR12 filler metal fractured by cleavage fracture in the HT HAZ at temperatures below the FATT of 70°C (table 4.5). At temperatures above the FATT temperature fracture occurred by ductile tearing in the HAZ. Figure 4.9 shows a section through a partially fractured specimen, which was tested at 74°C, with a ductile crack extending from the notch tip, through the HT HAZ, into the fine grained HAZ. The FATT curve is shown in figure 4.7b. The FATT temperature of 70°C, which was determined at a very sharp ductile-brittle transition, is therefore not the actual FATT of the HT HAZ since a completely brittle fracture occurred in this zone at 69°C (fig. 4.7b).

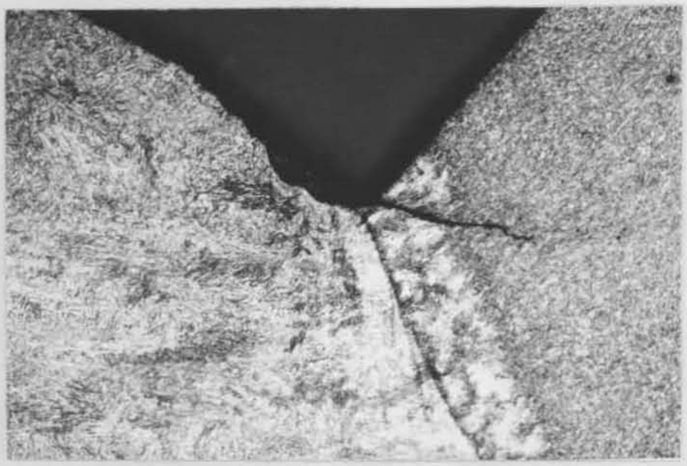

a.

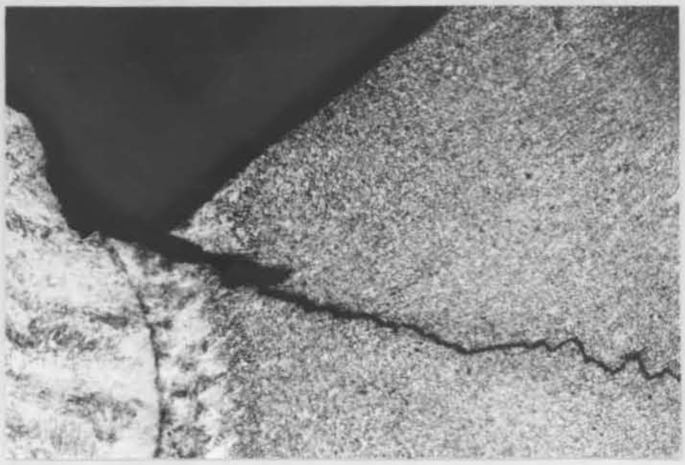

b.

Figure 4.9: Partially fractured hot rolled bead-on-plate 3CR12Ni bent specimens, welded with a E3CR12 filler metal and tested at 74°C.

a. Crack initiation

b. Crack propagation

The fracture mode transition at the FATT temperature of 69°C of the tempered 3CR12Ni specimens, welded with an AISI 316L weld metal, is similar to that of the hot rolled specimens welded with an E3CR12 filler metal (table 4.5). This may be attributed to the higher 316L weld metal strength (table 4.5) compared to that of the hot rolled specimens and the lower strength and fracture stress of the fine grained HAZ of the tempered specimens compared to that of the the hot rolled specimens.

3.2.2 3CR12 weld fracture behaviour

The actual FATT of the HT HAZ of the hot rolled 3CR12 bead-on-plate bend specimens, welded respectively with AISI 316L and E3CR12 filler metals were not determined, since the specimens fractured at temperatures below the FATT temperature by cleavage fracture (fig. 4.10) in the HT HAZ while 90° bends were achieved at temperatures above the FATT temperature. Plastic deformation occurred mainly in the low temperature HAZ (table 4.5 and fig. 4.11). Although the fracture stress of the HT HAZ is expected to be much lower than that of the adjacent fine grained HAZ and weld metal, this stress was never reached during bending at temperatures above the FATT temperature.

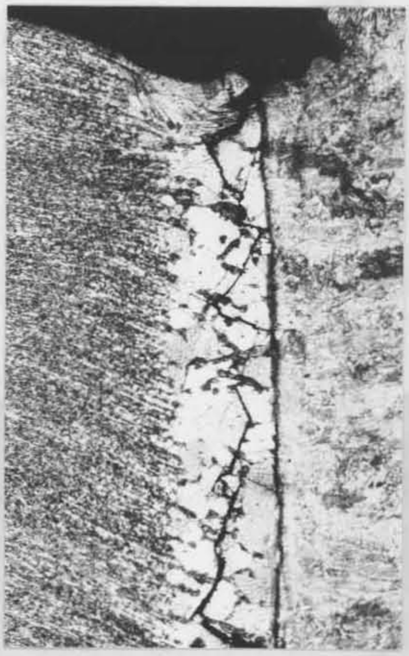

Figure 4.10: Partially fractured hot rolled bead-on-plate 3CR12 bent specimen welded with an E3CR12 filler metal. Specimen tested at 90°C. Note the plastic deformation lines at the notch tip preceding cleavage fracture (35X).

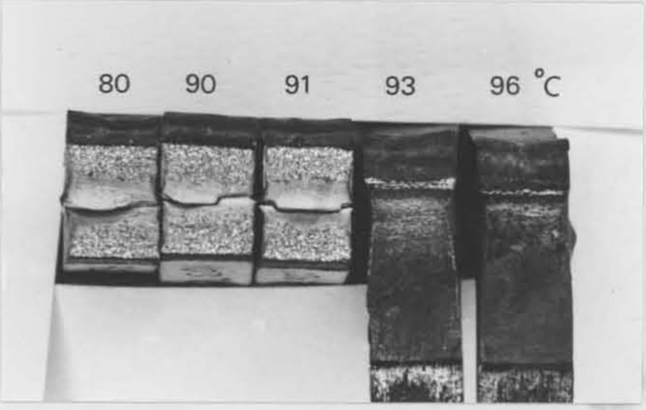

Figure 4.11: Fracture surfaces of hot rolled bead-on-plate 3CR12 bent specimens, welded with an AISI 316L filler metal. 90° bends were achieved at temperatures above the FATT while brittle cleavage fracture occurred in the HT HAZ at temperatures below 93°C. Test temperatures (°C) are also indicated.

A FATT of 105°C (table 4.5) was obtained for the tempered 3CR12 specimens, welded with a AISI 316L filler metal. This is again not the actual FATT of the HT HAZ since a fracture mode transition from cleavage fracture in the HT HAZ to ductile tearing in the low temperature HAZ occurred at the FATT temperature (fig. 4.12). The actual FATT will be much higher than 105°C even with the 35 percent martensite in this zone compared to the FATT of 92°C which was obtained for the hot rolled specimen with 15 percent martensite in the HT HAZ.

Two important observations can be made at this stage. First, the high FATT temperature or low fracture toughness which was obtained for the HT HAZ of 3CR12 even with 97 percent martensite in this zone and, secondly, the fact that the FATT temperatures, obtained with the bead-on-plate bend test, were not significantly influenced by the higher strength of both the hot rolled base metal or E3CR12 weld metal.

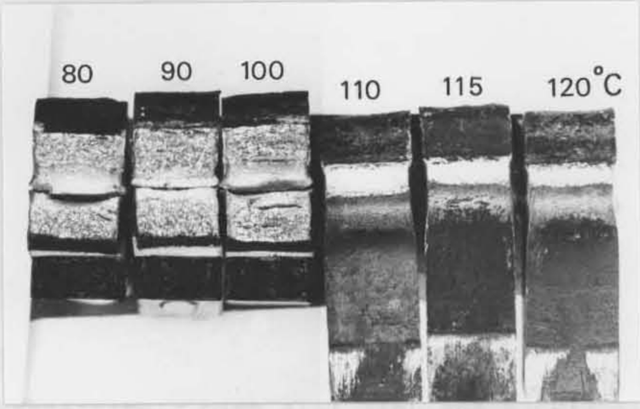

Figure 4.12: Fracture surfaces of tempered bead-on-plate 3CR12 bent specimens, welded with an AISI 316L filler metal. The test temperatures (°C) are indicated.

3.2.3 The influence of loading rate on the fusion line fracture behaviour behaviour of bead-on-plate welded 3CR12 and 3CR12Ni specimens

Figure 4.13 shows the influence of punch speed, ranging from 2 mm/min to 430 mm/min., on the FATT of the HT HAZ of bead-on-plate bend specimens which were prepared from hot rolled 3CR12 and 3CR12Ni plate, welded with AISI 316L and E3CR12 filler metals. The FATT temperatures obtained by impact loading in a Charpy impact machine are also indicated and summarized in table 4.5. Figure 4.13 shows that the FATT temperatures were not significantly influenced by punch speeds ranging from 2 mm/min to 430 mm/min. Higher FATT temperatures were obtained for the impact loaded specimens (table 4.5) except for the tempered 3CR12Ni specimens welded with an AISI 316L filler metal.

From the fracture mode transitions at the FATT indicated in table 4.5 it is evident that the actual FATT values of the HT HAZ were not determined with impact loading. The actual FATT of the HT HAZ of, e.g., tempered 3CR12 is therefore higher than the reported value of 106°C.

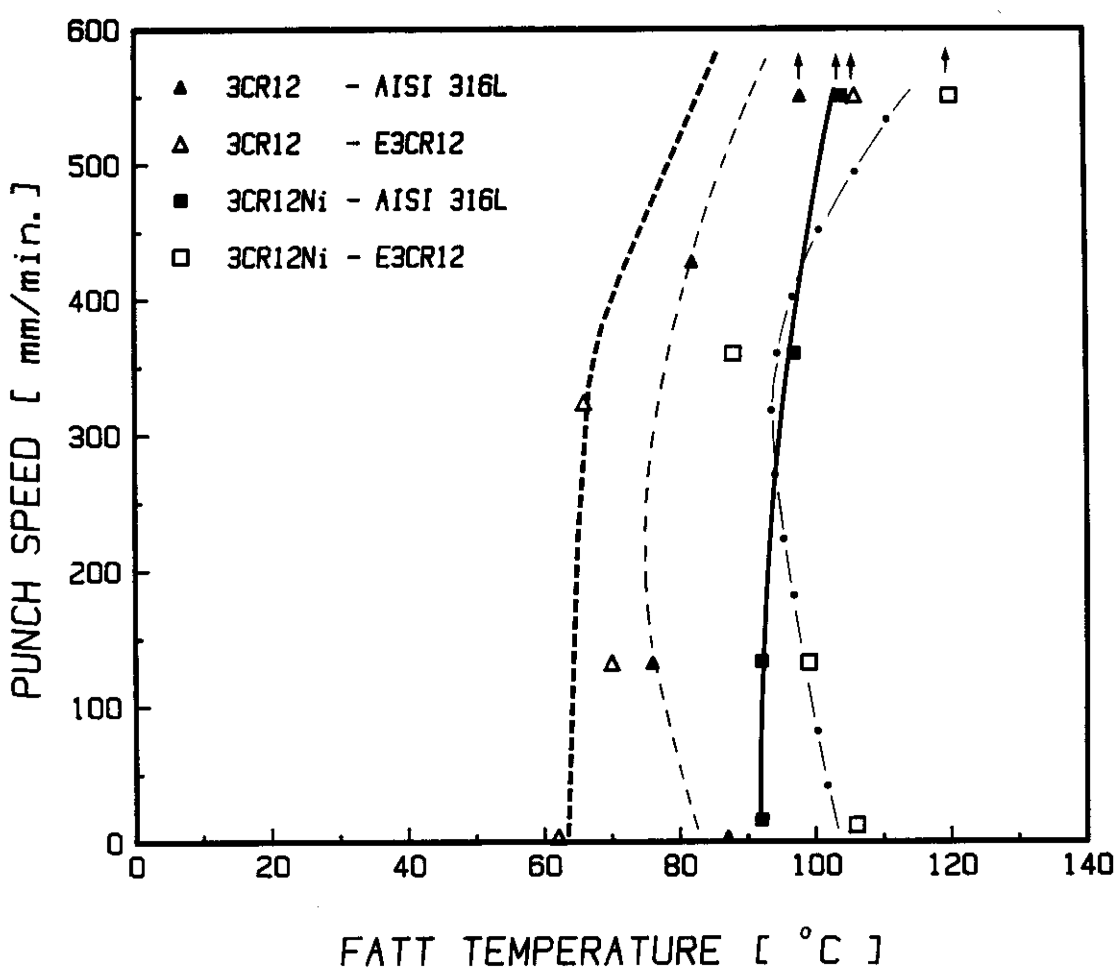

Figure 4.13: Loading rate (punch spead) versus FATT of the HT HAZ of hot rolled 3CR12 and 3CR12Ni bead-on-plate bent specimens, welded respectively with AISI 316L and E3CR12 filler metals. The FATT temperatures obtained by Charpy impact loading are indicated with arrows.

3.3 The influence of the fusion line orientation on the fracture behaviour of bead-on-plate bend specimens

Most of the FATT temperatures in table 4.5, which were obtained for welds on 6.2 mm 3CR12 and 3CR12Ni plate, are lower than the actual FATT temperatures of the HT HAZ since fracture occurred at temperatures above the FATT temperature by ductile tearing in the fine grained HAZ. This occurred among other factors as a result of the weld fusion line which is not oriented normal to the plate surface. The HT HAZ was therefore not subjected to the maximum bending tensile stresses during bend testing. Higher FATT temperatures will be obtained with the fusion line oriented normal to the plate surface since the HT HAZ will then be subjected to the maximum principal stress during bending.

The influence of the fusion line orientation on the FATT temperature of the HT HAZ of bead-on-plate bend specimens prepared from hot rolled 3CR12Ni plate (welded with E3CR12 filler metal) was therefore determined, and the results of this study is summarized in figure 4.14. Figure 4.15 shows sections through the welds of two test specimens with fusion line orientations relative to the plate surface of respectively 122° and 136°. The actual FATT (77°C) of the HT HAZ of only the hot rolled 3CR12Ni specimens welded with AISI 316L was determined (table 4.5). If the fracture stress of the fine grained HAZ is higher than the fracture stress of the HT HAZ of 3CR12Ni bend specimens, welded with E3CR12, then a FATT of approximately 77°C will be obtained with the weld fusion line oriented normal to the plate surface (fig. 4.14).

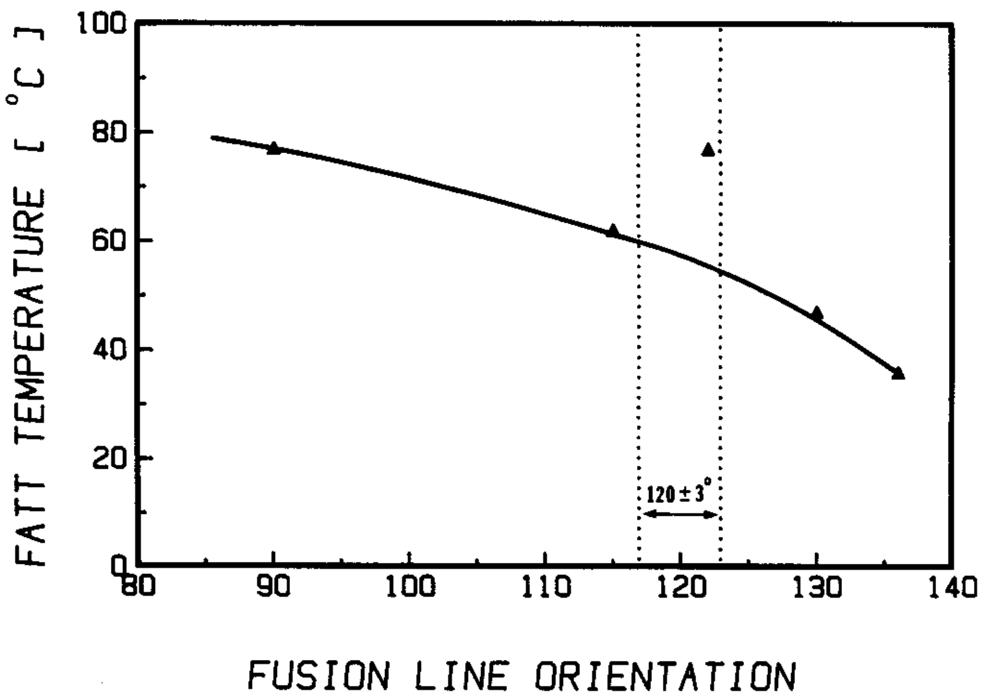

Figure 4.14: Fusion line FATT temperature versus fusion line orientation (θ in fig. 4.15) for hot rolled bead on plate 3CR12Ni specimens, welded with E3CR12. The FATT temperature at θ = 90° is an extrapolated value.

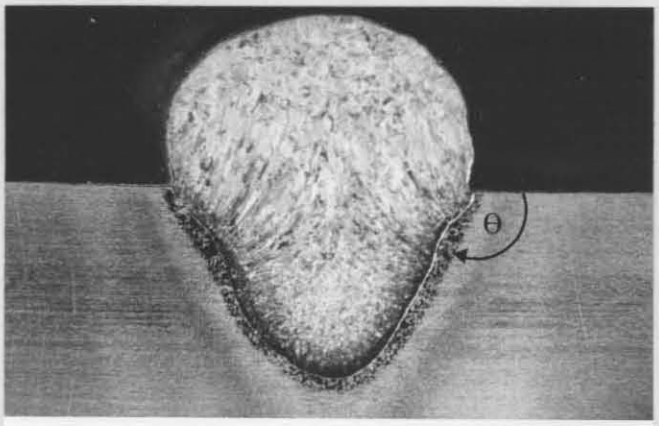

a.

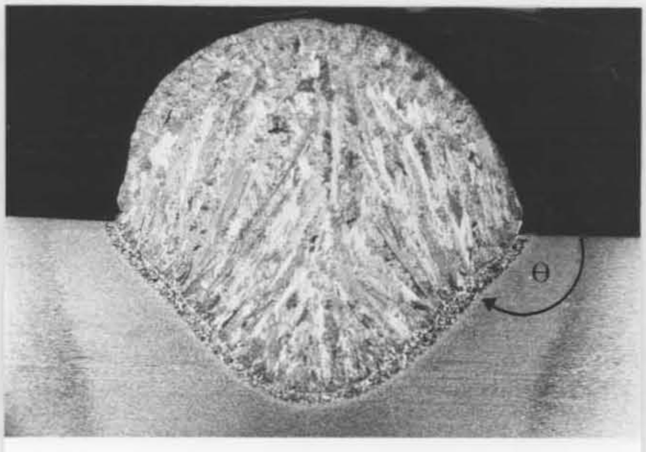

b.

Figure 4.15: Welds on bead-on-plate bend specimens with fusion line orientations relative to the plate surface of 122° (a) and 136° (b). Note the coarse grained HT HAZ adjacent to the fusion line.

Figure 4.14 shows that the fusion line FATT temperatures of bead-on-plate bend specimens is dependent on the fusion line orientation. The specimens which were used in this thesis to study the weld fusion line fracture behaviour of welds on 3CR12 and 3CR14 steels were therefore carefully selected, and only specimens with fusion line orientations within the range $120 \pm 3°$ were tested (fig. 4.14).

4. DISCUSSION

4.1 Fracture mode transition at the FATT

The fracture mode transitions which were observed at the FATT temperatures (table 4.5) of bead-on-plate welded 3CR12 and 3CR12Ni specimens may, be accounted for by using either the Cottrell-Petch or Davidenkov-Ludwik fracture theory. These theories are discussed in detail in chapter 2 and are used to explain the fracture mode transitions of welded 3CR14 steels in chapter 3.

Consider, e.g., the bead-on-plate bent specimens which were prepared from tempered 3CR12 plate (welded with a 316L filler metal) and which fractured by ductile tearing in the fine grained HAZ at temperatures above the FATT of 105°C, and by cleavage fracture in the HT HAZ at temperatures below 105°C (table 4.5). In order to explain this fracture mode transition in terms of the Davidenkov-Ludwik fracture theory, qualitative fracture and flow stress curves for respectively the fine grained HAZ, HT HAZ and weld metal are superimposed on the true stress-strain diagram in figure 4.16.

The relative positions of the different curves in figure 14.16 can be accounted for. The fracture stress curves E and A and the flow stress curve G for the fine grained HAZ is situated at higher stresses than the corresponding curves for the HT HAZ. This is due to the finer grain size and higher martensite content and hence higher fracture and flow stress for the fine grained HAZ compared to the HT HAZ. The weld metal flow stress curve H is situated at even higher stresses as a result of the relatively high weld metal strength (fig. 1.3 and table 4.5) and constraint offered by the large welding bead.

If the three different structures ahead of the notch tip of the bead-on-plate bend specimen represented in figure 4.16, are subjected to the same stress during bending at 90°C, a cleavage fracture will occur in the HT HAZ at a stress $\bar{\sigma}_1$, at the intersection of the curves D and F. The fracture stresses of the fine grained HAZ and weld metal are higher than this value. For any change in test temperature the relative shift of the different curves will always be such that the ductile fracture stress $\bar{\sigma}_2$ of the fine grained HAZ is higher than the cleavage fracture stress $\bar{\sigma}_1$ of

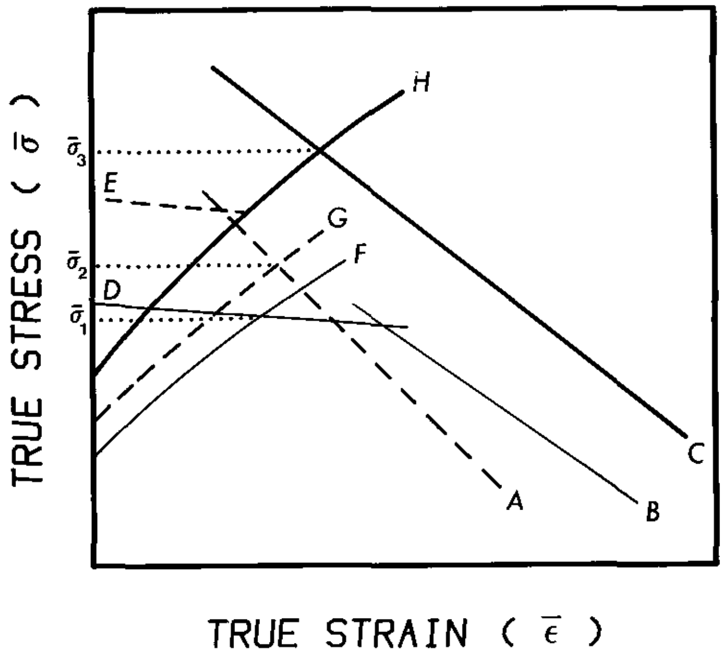

Figure 16: Fracture stress and flow stress curves for the fine grained HAZ, HT HAZ and weld metal at the notch tip of a bead-on-plate bend specimen, which was prepared from tempered 3CR12 plate welded with AISI 316L filler metal. The curves describe the crack tip stress-strain conditions of a specimen which is being bent at 90°C.

Curve A: Ductile fracture stress for the fine grained HAZ

Curve B: Ductile fracture stress for the HT HAZ

Curve C: Ductile fracture stress for the 316L weld metal

Curve D: Cleavage fracture stress for the HT HAZ

Curve E: Cleavage fracture stress for the fine grained HAZ

Curve F: Flow stress curve for the HT HAZ

Curve G: Flow stress curve for the fine grained HAZ

Curve H: Flow stress curve for the 316L weld metal

the HT HAZ. The fracture mode transition at the FATT of 105°C may then only be accounted for if the fine grained HAZ is subjected to higher stresses during bending than the HT HAZ and weld metal. With the weld fusion line of the bead-on-plate bend specimens not oriented normal to the plate surface and with the maximum principal stress developing a short distance ahead of the notch tip, due to plastic constraining, the fine grained HAZ will in fact be subjected to higher stresses during bending. A fracture mode transition from ductile tearing in the fine grained HAZ at 110°C to cleavage fracture in the HT HAZ at 100°C will then occur when the cleavage fracture stress $\bar{\sigma}_1$ of the HT HAZ is reached prior to reaching the ductile fracture stress $\bar{\sigma}_2$ of the fine grained HAZ.

The true FATT of the HT HAZ can only be determined when the fusion line is oriented normal to the plate surface. The different materials at the notch tip will then be subjected to the same stress during bending, with fracture occurring at any temperature in the HT HAZ due to both the relatively low brittle and ductile fracture stresses of this zone.

The fracture mode transition at the FATT (table 4.5) of the tempered 3CR12Ni specimens can also be explained in a similar manner. The fracture and flow stress curves will only be situated at higher stresses relative to the curves in figure 4.16.

The fracture mode transition from cleavage fracture in the HT HAZ to ductile fracture in the weld metal adjacent to the fusion line, which was obtained for the welded 14 percent chromium steels in chapter 3, was not observed for 3CR12Ni. This is probably due to the much higher weld metal strength (Vickers Hardness : 282) and therefore weld metal fracture strength of the 3CR12 specimens (compared to the 3CR14 specimens with a weld metal Vickers Hardness of 180). The high weld metal strength resulted from the formation of some martensite in the weld metal.

4.2 The influence of the weld and base metal strength on the FATT

Since the actual FATT of the HT HAZ of 3CR12 and 3CR12Ni could not be determined, it was not possible to obtain any conclusive results on the influence of the weld metal and base metal strength on the fusion line fracture behaviour of welds. Some of the FATT values in table 4.5 do indicate a slight increase of the HT HAZ FATT at higher base and weld metal strengths.

Another reason why no significant influence of the base and weld metal strength was observed on the FATT temperature, is the fact that the large welding bead alone offers a very high constraint to the weld HAZ during bending. In the next chapter the effects of the base and weld metal strength on the fracture behaviour of welds is demonstrated using bead-on-plate welded specimens with the large welding bead removed in order to eliminate the constraint associated with it.

It may be concluded therefore, that the newly developed bead-on-plate bend test is a very useful test for evaluating the influence of the narrow, coarse grained HT HAZ on the fusion line fracture toughness welds under conditions where the fracture behaviour of welds are primarily dependent on the fracture behaviour of the HT HAZ.

4.3 Fusion line FATT of 3CR12 and 3CR12Ni

Since 3CR12 was developed inter alia as a replacement for mild steel in various structural applications, the FATT of the HT HAZ of mild steel was also evaluated. Bead-on-plate bend specimens were prepared from 6.2 mm mild steel plate welded with an AISI 316L filler metal. Figure 4.17 shows the HT HAZ of a bead-on-plate weld on mild steel. A HT HAZ FATT

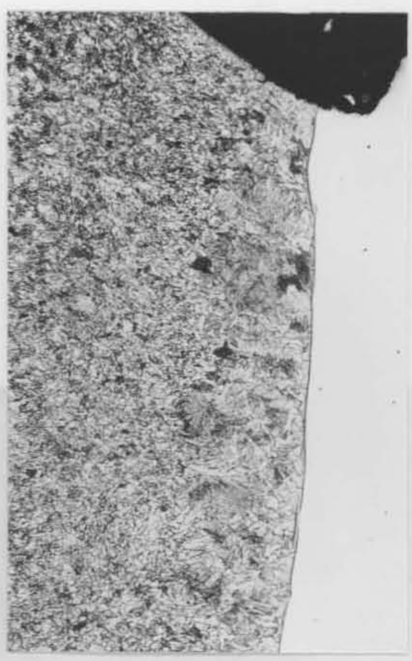

Figure 4.17: Weld HAZ microstructure of a bead-on-plate mild steel bend specimen. Note the fine grain size of the HT HAZ (35X).

of 0°C was obtained during slow bend testing with fracture occurring by ductile tearing in the low temperature HAZ at temperatures above 0°C.

The maximum fusion line FATT temperatures (table 4.5) which was obtained for 3CR12 and 3CR12Ni, are summarized in figure 4.18. Since a cleavage fracture occurred in the HT HAZ of both the 3CR12 and 3CR12Ni bead-on-plate bent specimens during impact loading at 100°C, it may be concluded that the Charpy ductile-brittle transition temperatures of the HT HAZ of both steels are probably higher than 100°C. These values are much higher than the transition temperatures of 0°C and 20°C which were reported for the HT HAZ of respectively 3CR12Ni and 3CR12 previously (8,9). This suggests that these low transition temperatures measured are in fact the transition temperatures for the tough fine grained HAZ adjacent to the HT HAZ. The most important observation at this stage is the fact that the HT HAZ FATT temperature of 3CR12 is higher than the value of 90-100°C which is reported for the HT HAZ of the ferritic stainless steel AISI 409, from which 3CR12 was developed(11).

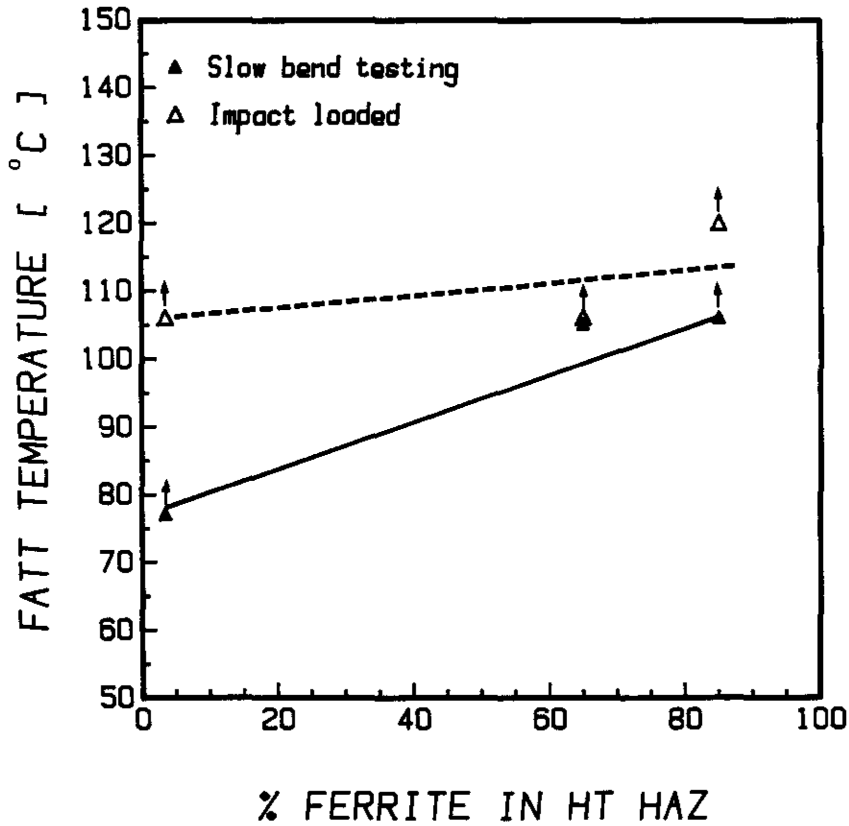

Figure 4.18: Maximum fusion line FATT temperatures obtained in this study for 3CR12 and 3CR12Ni bead-on-plate bend specimens.

Another important observation is the very small difference between the HT HAZ FATT values of the impact loaded 3CR12 and 3CR12Ni specimens (fig. 4.18). Although this difference is higher for the slow bend specimens, it is still relatively small. The toughness of the HT HAZ was therefore not improved to any significant extent by an increase in the martensite content from 15 percent to 98 percent. It seems to be insensitive to the marked reduction of the grain size from ASTM No. 1-2 to a fine grained, low carbon martensitic structure.

Therefore, it may finally be concluded that the toughness of the HT HAZ of 3CR12 is probably determined by other phenomena which have not yet been identified. The same effect was also observed in the previous chapter for the 14 percent chromium steels.

5. SUMMARY

a. The effect of the weld heat input of bead-on-plate welds on 11 mm 3CR12 plate, within the range 0.64 - 1.81 kJ/mm, was mainly to increase the width of the coarse grained HT HAZ from 0.41 mm to 1.10 mm; the phase composition and grain size are relatively unaffected.

b. The fusion line FATT of both 3CR12 and 3CR12Ni bead-on-plate bend specimens were not significantly changed by an increase of the punch speed during bending from 2 mm/min to 430 mm/min. Slightly higher transition temperatures resulted when the specimens were tested by impact loading in a Charpy machine.

c. The fusion line FATT of bead-on-plate bend specimens is dependent on the fusion line orientation relative to the plate surface. Only specimens with fusion line orientations within the range 120 $\pm 3°$ were tested.

d. The influence of the weld metal strength on the fusion line fracture behaviour of bead-on-plate welds on 6.2 mm 3CR12 plate may not be determined using the newly developed bead-on-plate bend test. This is attributed to the high constraint offered alone by the large welding bead.

e. The actual FATT of the HT HAZ of bead-on-plate MIG welds on 6.2 mm 3CR12 and 3CR12Ni plate could not be determined due to the fracture mode transition at the FATT from cleavage fracture in the HT HAZ to ductile tearing or bending in the fine grained and low temperature HAZ. This fracture mode transition is explained in terms of the Davidenkov-Ludwik fracture theory.

f. Maximum FATT temperatures of respectively 77°C and 106°C were obtained, during slow bend testing, for the HT HAZ of bead-on-plate welds on 3CR12Ni and 3CR12 plate. These temperatures increased to 106°C for 3CR12Ni and 120°C for 3CR12 when the bend specimens were impact loaded in a Charpy machine.

g. A FATT of 0°C was obtained for the HT HAZ of bead-on-plate welded mild steel specimens, prepared from 6.2 mm mild steel plate.

h. The fracture toughness of the HT HAZ of 3CR12 is much lower than either of the values reported in literature for the weld HAZ's of 3CR12 and AISI 409 from which 3CR12, was developed.

i. The fracture toughness of the HT HAZ of 3CR12 was not significantly improved by an increase in the martensite content from 15 percent to 98 percent.

j. It is finally concluded that since the fracture toughness of the HT HAZ of 3CR12 is not dependent on the martensite content and grain size, it is probably determined by other phenomena which have not yet been identified.